Numerical study on the movement of air inside the inner cavity of a hovercraft model

M S Pavăl[1], A Popescu[1], T Popescu[2], D Zahariea[2] and D E Husaru[3]

[1]Mechanical Engineering and Road Automotive Engineering Department, "Gheorghe Asachi" Technical University of Iași, Iași, Romania
[2]Fluid Mechanics, Fluid Machinery and Fluid Power Systems Department, "Gheorghe Asachi" Technical University of Iași, Iași, Romania
[3]Mechanical Engineering, Mechatronics and Robotics Department "Gheorghe Asachi" Technical University of Iasi, Iasi, Romania

E-mail: pavalmihaisilviu@gmail.com

Abstract. This article describes several numerical simulations on aerodynamic characteristics of an oval shaped hovercraft. The 3D model was created in CATIA V5 and numerical analysis was performed in ANSYS Fluent. For numerical simulation, the velocity at inlet section and air-clearance height were specified as input parameters, with stationary hovercraft, flat ground surface and the flexible skirt that does not deform under the influence of the pressure created as imposed conditions. Three different air-clearance heights and velocities at inlet section are analysed. The output results of the numerical simulations are mass flow rate, lift force, static pressure, velocity distribution and pressure inside hovercraft.

1. A brief introduction about advanced marine vehicles

Since ancient times, people have been fascinated by the possibility of crossing land and water in a relatively short time, as these civilizations developed settlements near the watercourses. In order to achieve the economic growth of an ancient civilization, it was necessary to perform trade, navigation being a decisive factor.

Over time, the concept of transport has developed from ancient civilization boats to sophisticated vessels equipped with advanced equipment, such as advanced marine vehicles.

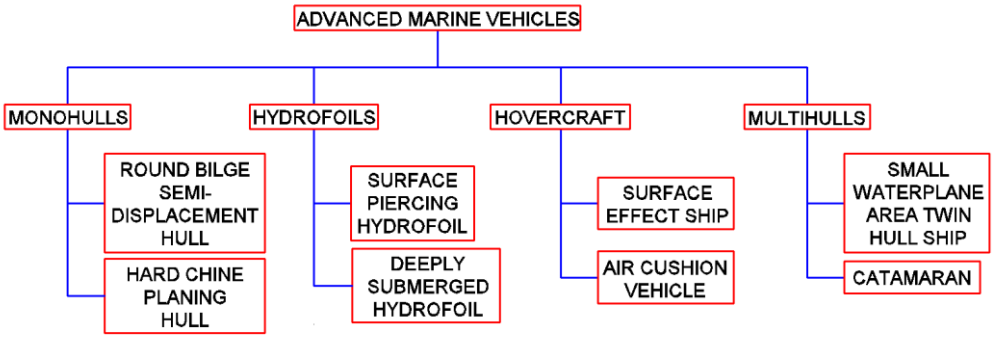

Figure 1. Classification of Advanced Marine Vehicles.

To better understand the classification of these vehicles (figure 1), the sustension triangle will be used, as detailed in figure 2. All three corners of the triangle specify different properties for the three types of lift forces:

- the top of the triangle represents hydrostatic buoyancy,
- in the bottom right represents hydrodynamic lift,
- in the bottom left represents aerostatic lift, [1].

With this sustention triangle, new hybrid vehicles may be defined, depending on the characteristics required in the design stage. The subject of this paper is focused on aerodynamic study inside the inner cavity of an advanced marine vehicle, the hovercraft.

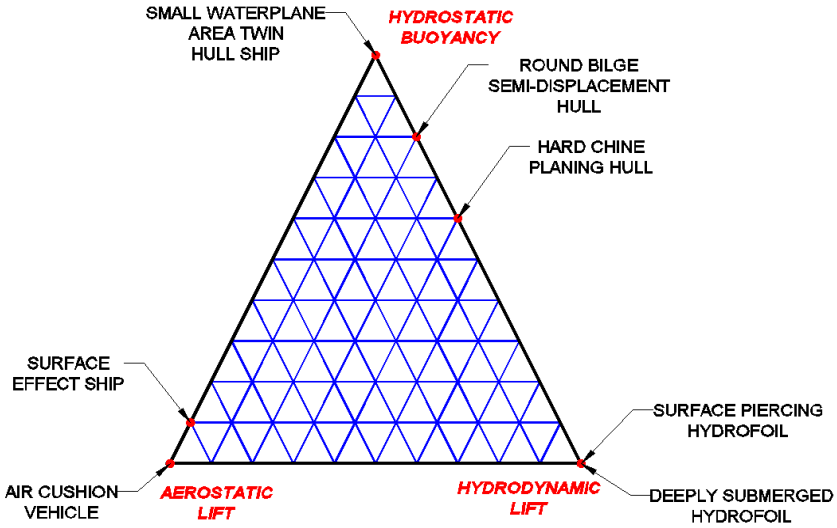

Figure 2. Sustention triangle (adapted from [2]).

2. Introduction on hovercrafts

Hovercrafts are vehicles designed to run on different types of surfaces such as: ground, water, ice, sand, swamps - generating amphibious qualities in this type of vehicles. Another important feature of hovercraft is higher speeds comparing with some conventional ships, [3].

Although it is reported that this concept was first proposed by John Thornycroft in 1870, [4], the concept of air-cushion vehicles was born earlier, namely in 1716. The Swedish Emanuel Swedenborg proposed such a prototype and his idea was presented in the fourth edition of Daedalus Hyperboreus journal, [5].

The first hovercraft prototype was made in 1956 by the British engineer Christopher Cockerell. In 1959, his experimental hovercraft crossed the English Channel (more precisely the distance between Dover and Calais), thus marking the beginning of the evolution of air cushion vehicle, [6].

Hovercrafts are vehicles under continuous development, designed for particular to unique applications. These vehicles are used in places where other conventional vehicles could not reach, this being their main advantage. Several areas for hovercraft applications include their use as icebreakers, defence and security, rescue and humanitarian aid, energy sector and logistics etc., [7].

3. Main components of a commercial hovercraft

The evolution of these types of vehicles was stimulated by intense studies carried out in order to find military applications. Over time, constructive changes have been developed for hovercrafts in order to improve their performances.

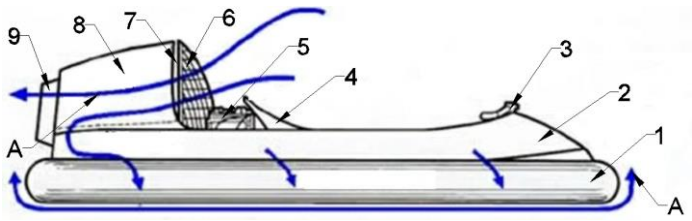

Figure 3. Main components of a commercial hovercraft (adapted from [8]) A - airflow, 1 - skirt, 2 - hull base, 3 - steering wheel, 4 - seat, 5 - engine, 6 - fan / propeller cover, 7 - fan or propeller (inside 8), 8 - ventilation duct and 9 - rudders.

4. Working principle of a hovercraft

Hovercrafts are vehicles that travel using an air cushion that is located between the lower hull base and the running surface. Depending on the method used to achieve lift and thrust force, the hovercrafts are classified into two types of different configurations.

The first configuration includes only a fan or propeller, to produce both the necessary lift and thrust force required by the hovercraft to move above various surfaces. Its constructive shape is based on a structure that has two ducts: part of the air is sent into flexible skirt through one duct while the rest is sent through the rudders, figure 3.

A second configuration type for hovercrafts consists of two fans or a fan and a propeller, where one of the fans develops the lift force, while the second fan or propeller achieves the necessary thrust force.

The working principle of a hovercraft is based on a stream of air, produced by fan perpendicular or at a certain angle to the structure and directed under the hull to achieve the necessary lift force. After a short period of time it can be noticed that the flexible skirt deforms until there is some air leakage at the periphery. It can be noticed that vehicle rises from the ground due to the air cushion created under the hull. When designing these types of vehicles, the fan is selected to provide the amount of air necessary to maintain the air-clearance height. Generally, the air-clearance height that is measured with the entire system in operation, has values between 200 and 600 millimetres, [9].

The idea of building such vehicles takes advantage of two major benefits of the air cushion: vehicle suspension and lubricating, [10]. Using air cushion instead of classic wheels, the friction encountered while driving is significantly reduced, which is an important asset.

The hovercraft control mechanism includes a lever or a manoeuvre wheel that acts on rudders located at the outlet of the ventilation duct. This duct has two functional roles: to protect the thrust system and to ensure a uniformity of the streamlines that enter into the rudders.

With regard to hovercraft steering, it can be noticed that the right-hand turn is done by orienting the rudders to the left and the left-hand turning is done by orienting the rudders to the right, [11].

5. The main components of the hovercraft proposed for study

The main hovercraft components include: hull, flexible skirt and supporting elements. The 3D model was made in the CATIA V5. Aluminium has been chosen for the hull, and rubber was chosen for flexible skirt. The main components of the hovercraft are presented in figure 4 and the overall dimensions of the proposed model are shown in figure 5.

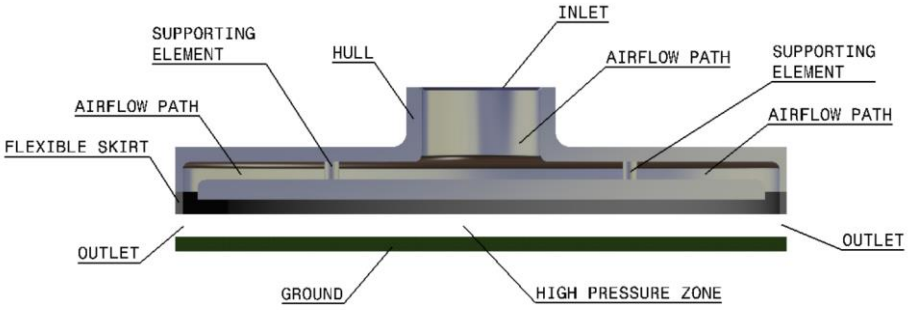

Figure 4. Particularities of the constructive model.

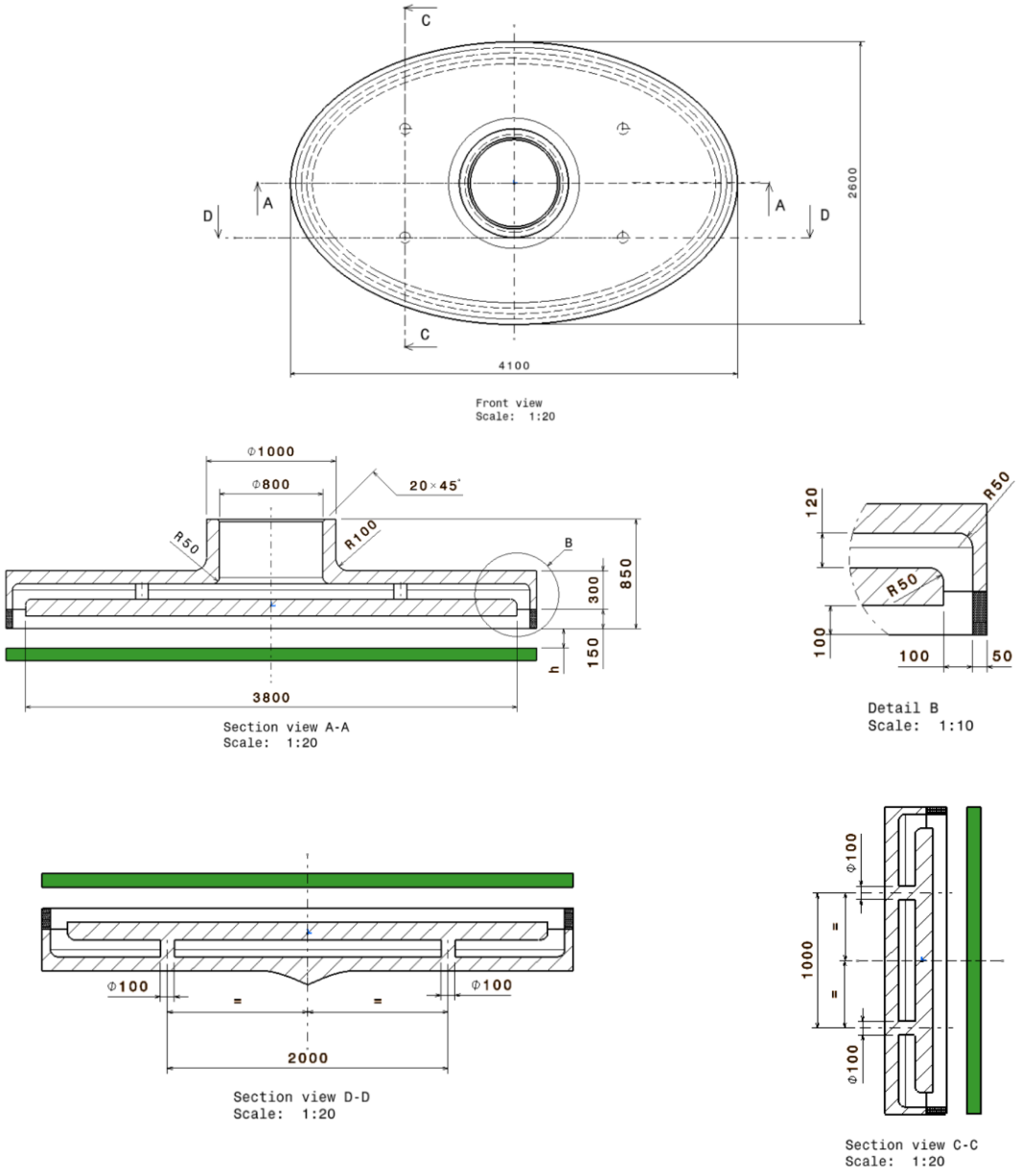

Figure 5. Geometry model with the corresponding dimensions.

6. Numerical analysis

The numerical simulations have been performed using ANSYS Fluent. For air-clearance height two values were used, h_1=30 mm and h_2=50 mm, and for each value, three input section air velocity have been considered, v_1=25 m/s, v_2=30 m/s and v_3=35 m/s.

The CFD analysis steps are:

- Geometry setup: at this stage the 3D model has been imported and the fluid volume on which the simulation will be made has been defined, figure 6.

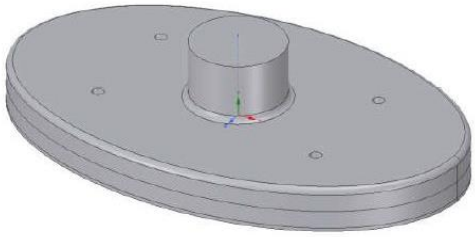

Figure 6. The fluid volume.

- 3D mesh setup: the generated mesh has 625697 nodes and 3263260 elements, figure 7. The mesh was considered to be the one generated by the program, intervening to improve it only in the connection areas and in the area of supporting elements of the upper part of the hull. The mesh quality is defined using skewness parameter, figure 8. Regarding the skewness parameter, it can be defined as the deviation between the real shape of a finite element and its ideal shape, considering that the ideal shape is an equilateral triangle for the finite elements of triunghiular type, respectively a rectangle for finite element of the quadrilateral type.

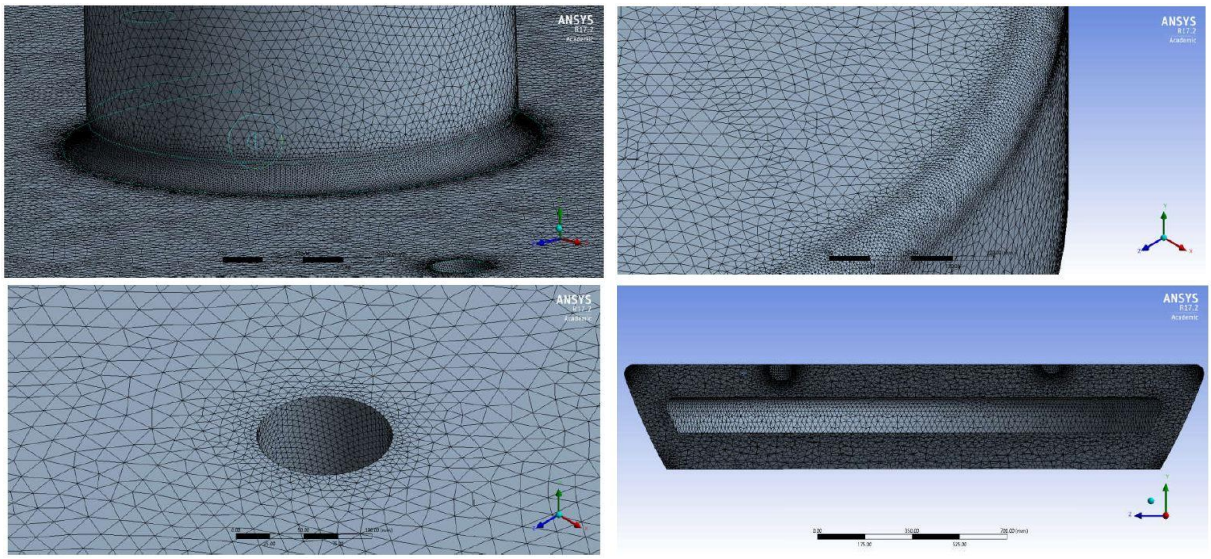

Figure 7. Mesh density.

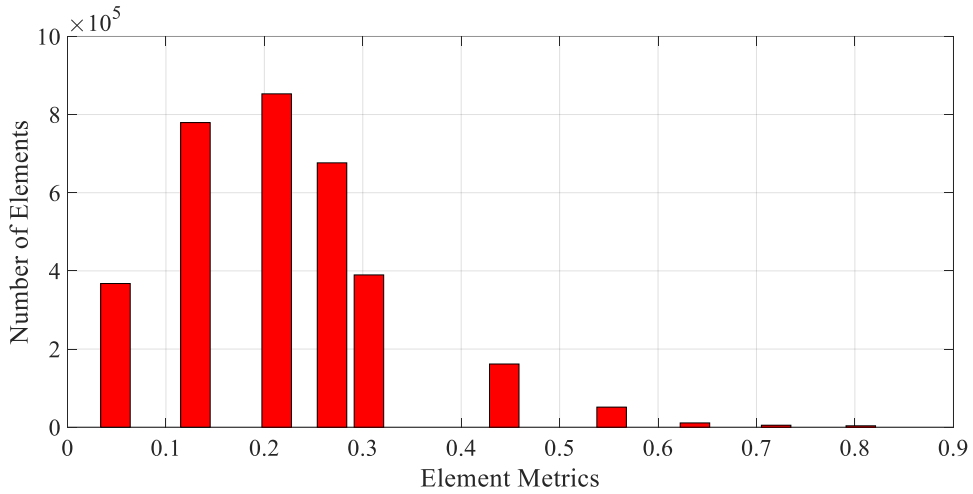

Figure 8. Skewness parameter that relates to mesh quality.

- Defining parameters:
  - checking the mesh
  - defining the solution model: particular model chosen is shown in figure 9
  - material: air
  - setting the boundary conditions: the velocity in the inlet section and the pressure at the outlet section
  - defining residuals and mass flow rate
  - run calculation for 1000 iterations.

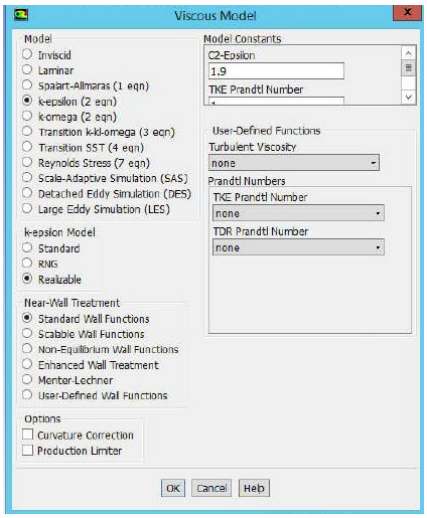

Figure 9. Solving model parameters.

7. Simulation results

To obtain the solution convergence, a number of 1000 iterations proved to be sufficient, as presented in figure 10, for (a) mass flow rate, (b) lift coefficient and (c) residuals.

The most important parameters for hovercraft performance analysis obtained by numerical simulation are presented in figure 11: (a) velocity distribution, and (b) gauge pressure distribution.

The velocity vector field is presented in figure 12 and 3D streamlines are presented in figure 13. All these results are referring to the study case defined by h_1=30 mm and v_1=25 m/s.

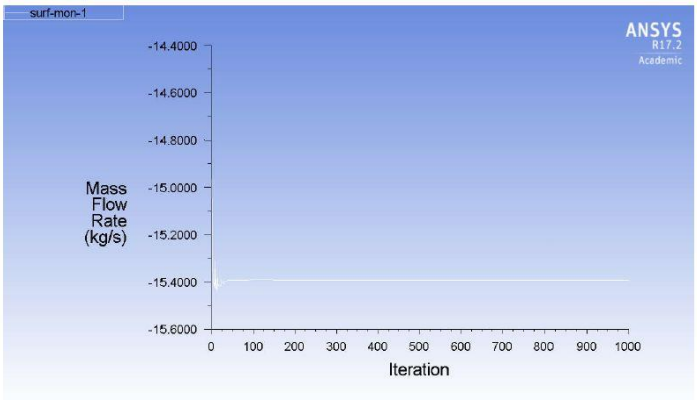

(a)

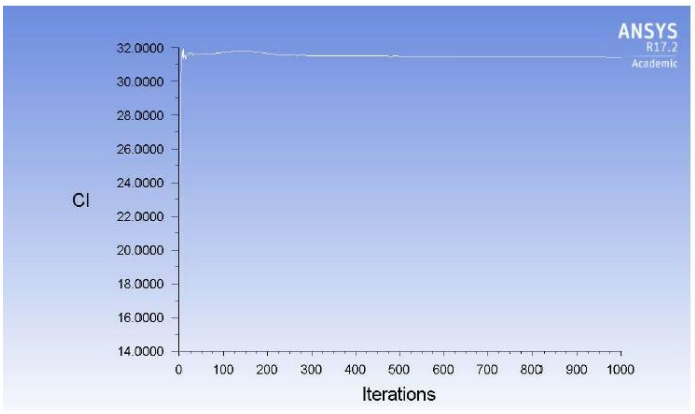

(b)

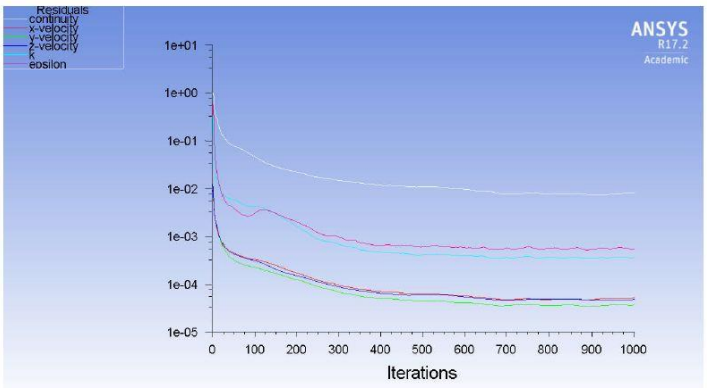

(c)

Figure 10. Mass flow rate (a), coefficient of lift force (b), and residuals (c).

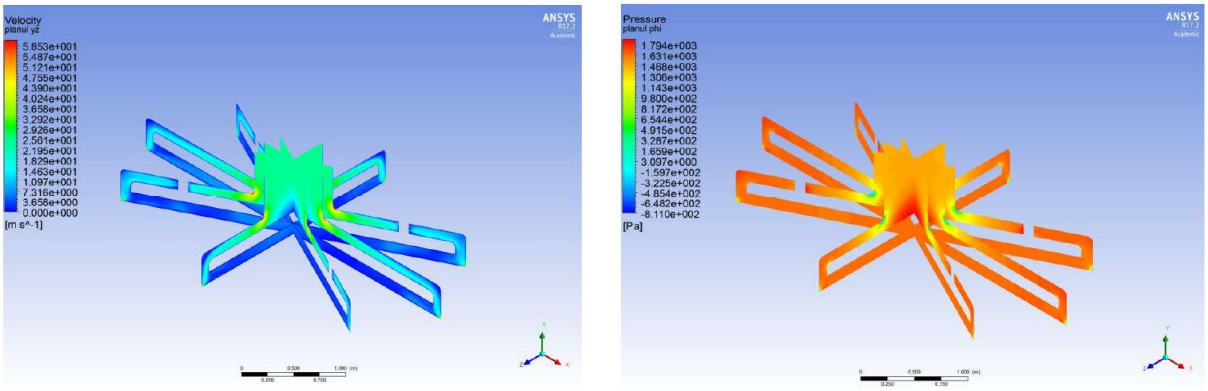

(a) (b)

Figure 11. Velocity distribution (a), and gauge pressure distribution (b).

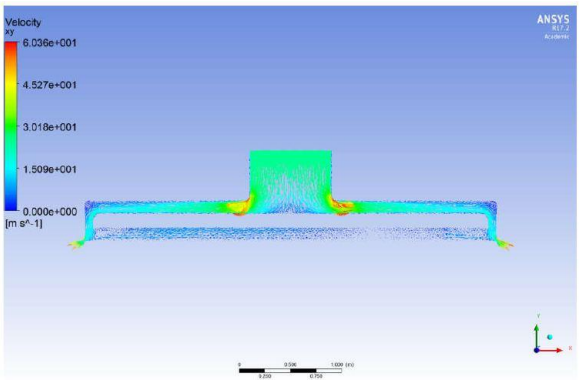

Figure 12. Velocity vector field.

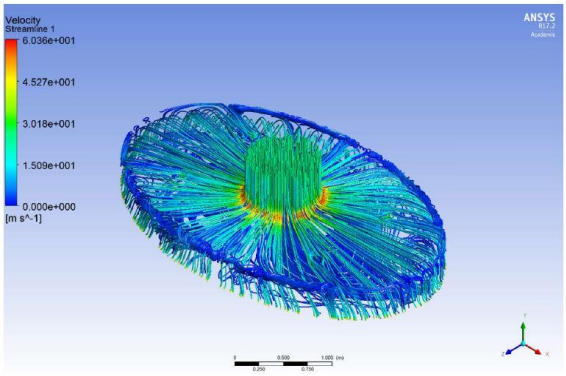

Figure 13. 3D streamlines.

The boundary conditions are: for the input section velocity v_1, v_2 and v_3 are required and the output section requires the gauge pressure with zero Pascal value. Gauge pressure is determined according to the reference pressure, atmospheric pressure p_a=101325 Pa.

The numerical results are presented in table 1: input parameters (air-clearance and air velocity) and output parameters (lift force, static pressure and mass flow rate).

Table 1. Parameters results from simulation.

No	Input parameters		Output parameters				
	Air-clearance height h [mm]	Air velocity v [m/s]	Lift force F_s [N]	Static pressure - inlet p_{inlet} [Pa]	Input mass flow rate Q_{inlet} [kg/s]	Output mass flow rate Q_{outlet} [kg/s]	Overall mass imbalance $Q_{overall}$ [%]
1	30	25	12031.55	1470.35	15.392117	-15.392112	0.000032
2		30	17339.86	2111.46	18.47054	-18.470561	0.00011
3		35	23597.82	2868.40	21.548963	-21.548992	0.00013
4	50	25	4360.95	424.98	15.39213	-15.392137	0.000045
5		30	6280.63	607.89	18.470556	-18.47057	0.000075
6		35	8546.38	822.42	21.548982	-21.548987	0.000023

It can be seen in table 1 that the output mass flow rate have a negative value due to the orientation of the velocity vector with respect to normal surface vector.

In figure 14 the 2D streamlines for the ground boundary are presented for all six case studies analysed:

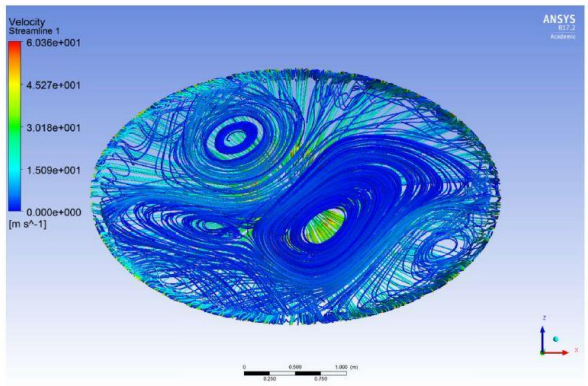

(a) h_1=30 mm and v_1=25 m/s

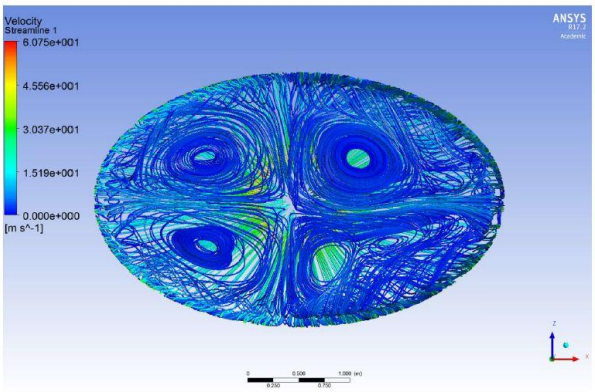

(d) h_2=50 mm and v_1=25 m/s

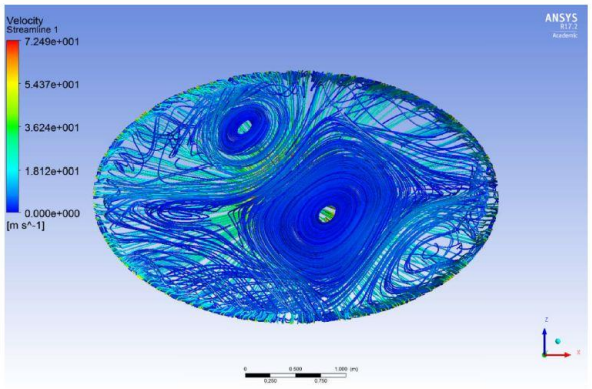

(b) h_1=30 mm and v_2=30 m/s

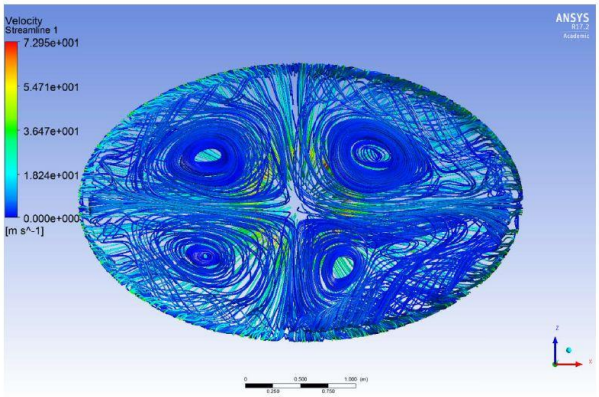

(e) h_2=50 mm and v_2=30 m/s

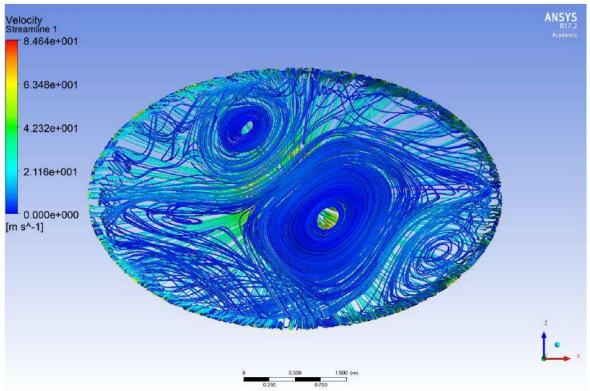

(c) h_1=30 mm and v_3=35 m/s

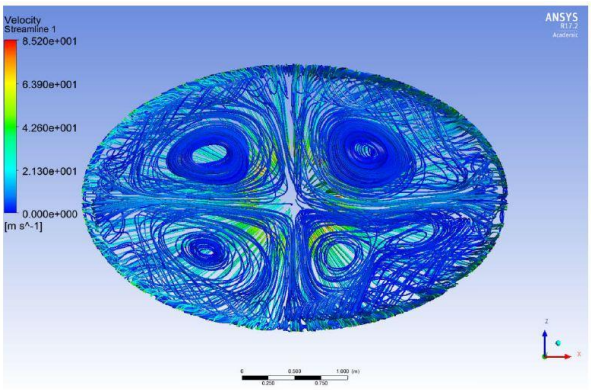

(f) h_2=50 mm and v_3=35 m/s

Figure 14. 2D streamlines.

8. Conclusions

In recent years, finite element analysis plays an important role in engineering, being a tool used in prototypes and products development in various fields of engineering. For the specific case presented in this paper, numerical simulations were used to determine the values of several parameters such as: lift force, mass flow rate, gauge pressure distribution, velocity vectors, and streamlines, which may help to improve the prototype by resizing components, in order to obtain optimal operational lift force and proper stability.

From numerical values obtained, it can be inferred that increasing the air-clearance, for the same air velocity, static pressure and lift force decrease. Moreover, for the same air-clearance height, the lift force increases with respect to the air velocity: by 96.13% for h_1=30 mm, and by 95.97% for h_2=50 mm, while the air velocity increases from 25 m/s to 35 m/s. Referring to static pressure, it can be observed that for the same air-clearance height, this pressure increases with respect to the air velocity by 95.08 % for h_1=30 mm and by 93.51% for h_2=50 mm, while the air velocity increases from 25 m/s to 35 m/s.

According to the numerical values presented in table 1, for all six cases studied, the inlet airflow has the same approximate value as the outlet flow, which is a consequence of the continuity equation.

The overall mass imbalance is also presented in table 1; all the values are less than 1%, thus the overall mass conservation being satisfied.

With regard to the representation of the velocity vectors, the highest air velocities are encountered in the area of the connection radius R=50 mm (section view A-A from figure 5) and at the periphery of flexible skirt (figure 12). On the area where the four supporting elements are located, can be seen that there are small air velocities around them. By correlating with representation of the gauge pressure inside the hovercraft, the small pressures (both positive and negative values) meet also at the radius R=50 mm and at the periphery of the flexible skirt (figure 11b). The 2D streamlines trajectory presented in figure 14 indicates that there are energy losses in areas where vortices are formed.

To obtain more accurate results related to the parameters mentioned above, different strategies may be considered: improving the mesh quality and increasing the number of iterations.

9. References

[1] Yun L and Bliault A 2012 *High Performance Marine Vessels* (New York: Springer-Verlag)
[2] Overview of High - Performance Vehicles as Naval Platforms - Volker Bertram http://slideplayer.com/slide/3571207/ (accessed on 04.03.2018)
[3] Noor Mohamed S H, Syam K, Jaafar A A, Sharif Mohamad M F, Ghazali M R, Ibrahim W I and Atan M F 2016 Development of a working Hovercraft model *IOP Conference Series: Materials Science and Engineering* **114** *012150*
[4] Jaiswal R, Bhardwaj R, Anant R, Sen P K and Bohidar S K 2014 A Study about hovercraft *IJSRD - International Journal for Scientific Research & Development* **2** pp 344-7
[5] McPeake M 2004 A Research Paper on the History of the Hovercraft http://hovertron.tripod.com/images/mpaper.pdf (accessed on 04.03.2018)
[6] Amiruddin A K, Sapuan S M and Jaafar A A 2008 Analysis of glass fibre reinforced epoxy composite hovercraft hull base *Materials and Design* **29** pp 1453-8
[7] GriffonHoverwork - http://www.griffonhoverwork.com/applications.aspx (accessed on 05.03.2018)
[8] About Hovercraft. How Does it Work? http://www.discoverhover.org/abouthovercraft/works.htm (accessed on 04.03.2018)
[9] Okafor B E 2013 Development of a Hovercraft Prototype *International Journal of Engineering and Technology* **3** pp 276-81
[10] Sharma R C, Dhingra M, Pathak R K and Kumar M 2014 Air cushion vehicles: configuration, resistance and control *Journal of Science* **4** pp 667-73
[11] Shrirao R R, Kale S P, Rakhde D K and Khot A S 2016 Design & Fabrication of ACV *International Journal of Emerging Trends in Science and Technology* **3** pp 3995-4015

Acknowledgments

The authors would like to acknowledge the technical resources offered by the Laboratory of Computer-Aided Fluid Engineering, from the Department of Fluid Mechanics, Fluid Machinery and Fluid Power Systems, The "Gheorghe Asachi" Technical University of Iasi, Romania. The Laboratory of Computer-Aided Fluid Engineering has been equipped with technical resources with the financial support of the grant ENERED, POSCCE-A2-O2.2.1-2009-4, ID 911.